Available online at www.sciencedirect.com

ScienceDirect

IFAC PapersOnline CONFERENCE PAPER ARCHIVE

IFAC PapersOnLine 58-20 (2024) 487–492

Disturbance Observer Based Control for a Remotely Operated Vehicle

A. Baldini * **R. Felicetti** * **A. Freddi** * **A. Monteriù** *

* *Department of Information Engineering, Università Politecnica delle Marche, Via Brecce Bianche, 60131 Ancona, Italy, (e-mail: {a.baldini, r.felicetti, a.freddi, a.monteriu}@univpm.it)*

Abstract: This paper presents a Disturbance Observer Based Control scheme which deals with the full pose tracking control problem of a Remotely Operated Vehicle. The uncertainties are lumped, estimated by a Nonlinear Disturbance Observer and feed-forwarded in a tracking controller. The solutions only relies on known quantities, providing a dynamic disturbance compensation and ultimately bounded errors. The order of the disturbance observer is a design parameter, which is able to provide additional integral actions. Finally, numerical simulations test the proposed technique.

Keywords: Disturbance Observer Based Control, Remotely Operated Vehicle.

1. INTRODUCTION

Remotely Operated Vehicles (ROVs) operate in challenging environments characterized by various environmental disturbances, including waves and ocean currents. Traditional dynamic positioning control strategies have been developed to effectively filter out the modal frequency of waves, preventing the vehicle from counteracting these disturbances (Fossen, 1994). This approach is designed to avoid issues such as actuator saturation and wear-and-tear. However, certain applications, such as manipulation tasks or close-quarters visual inspection, require a higher level of precision in position and orientation control (Walker et al., 2021). In these specific scenarios, the limitations of traditional control methods become evident. Hence, there is a need to refine the ROV's control system for effective disturbance rejection and enhanced precision.

The Disturbance Observer Based Control (DOBC) has proved to be an effective method to deal with disturbance rejection in many fields of application (Chen et al., 2016). It makes use of an observer for the estimation of a lumped disturbance, which can be the outcome of several contributions, like external disturbances (Ahmed et al., 2020), parameters uncertainties (Benevides et al., 2022), model mismatching, etc. The observer design method could follow several approaches, like extended state observers (Guo and Zhao, 2011) and sliding mode observers (Yang et al., 2012). In particular, in DOBC, a Nonlinear Disturbance Observer (NDO) is designed as a reduced order observer (Guo and Chen, 2005). Recently, the disturbance observer based paradigm has been heavily investigated for marine systems (Gu et al., 2022; Baldini et al., 2022b). Indeed, there are lots of undesired and unknown effects to deal with, including the estimation of the cable effect (Li et al., 2018) and the estimation of faults effect (Baldini et al., 2018a; Liu et al., 2018; Hosseinnajad and Loueipour, 2021; Baldini et al., 2022a; Hosseinnajad and Loueipour, 2023). Depending on the lumped disturbance, several observers methods have been investigated, including neural network based disturbance observers (Chu et al., 2016, 2021) and sliding mode based disturbance observers (Guerrero et al., 2020; Gao et al., 2019). The agile design of a DOBC has been used to couple observers with several composite controllers. In Oliveira et al. (2021) a disturbance observer is coupled with model predictive control. In Chen et al. (2019); Mu et al. (2021) disturbance observers are coupled with sliding mode control, while an extended state observer is coupled with integral sliding mode control in Cui et al. (2017).

The objective of this paper is to design a DOBC scheme to solve the trajectory tracking problem for an over-actuated ROV with 6 degrees of freedom (i.e., position and attitude). The internal NDO is designed with no assumption on the external marine current, expect of being mainly composed by low frequency components. Compared to the model-based methods in the literature, that require a good knowledge of the system parameters, the proposed disturbance estimation requires minimal modeling effort (no need to estimate added masses, hydrodynamic coefficients, etc.) and relies on known parameters only. In fact, the proposed strategy lumps together all the spurious terms involving hydrodynamics, so that only gravity, buoyancy, and actuator thrust estimations are actually needed for closed loop control.

2. ROV MODEL SUMMARY

In this Section, we briefly introduce the model of the BlueROV 2 Heavy (Wu, 2018) which represents the case study, where we introduce the effects of the marine current, and we detail the input mapping.

Following the standard approach (Fossen, 1994), a body fixed frame R_b (centered in the center of mass) and a (assumed inertial) earth fixed frame R_e are considered. Then, let us define the variables $\eta = col(p, \Omega)$, $\nu =$

10.1016/j.ifacol.2024.10.101

$col(v^b, \omega)$, where $col(p, \Omega)$ denotes $\begin{bmatrix} p^T & \Omega^T \end{bmatrix}^T$. In detail, η includes the position $p = col(x, y, z)$ and orientation $\Omega = col(\varphi, \theta, \psi)$ vectors in the inertial earth-fixed frame, ν includes the linear (v^b) and angular (ω) velocities vectors in the body-fixed frame. The xyz-convention is used for the rotation matrix

$$R_b^e(\eta) = R_z(\psi) R_y(\theta) R_x(\varphi) \tag{1}$$

from R_b to R_e, defining then φ, θ, and ψ as the pitch, roll, and yaw angles. The subsequent kinematic angular coordinate transformation (see Fossen (1994) for further details) is denoted with $T(\eta) \in \mathbb{R}^{3\times3}$, hence $\dot{\omega} = T(\eta)\Omega$. The well known model for marine vehicles from Fossen (1994) is employed to model the dynamics of the ROV

$$\begin{aligned} &\dot{\eta} = J(\eta)\nu \\ &(M_{rb} + M_a)\dot{\nu} + (C_{rb}(\nu) + C_a(\nu))\nu + D(\nu)\nu + g(\eta) = \tau, \end{aligned} \tag{2}$$

where $J(\eta) = \text{diag}\,(R_b^e(\eta),\, T(\eta))$ is the overall kinematic transformation and diag$(\cdot)$ returns a block diagonal matrix with the arguments on the main diagonal. The following assumptions are considered.

A_{I}: The ROV exhibits low speed movements.
A_{II}: The marine current shows relatively slow dynamics.
A_{III}: The ROV is symmetric w.r.t. the body axes.

The restriction to low speed movements and slow marine current variations allow us to neglect the effects of turbulent flow. We note that the ROV speed is limited in many practical applications (Fossen, 1994), however, it represents a limitation in case of turbulent marine currents. Assuming the symmetry of the ROV makes it possible to neglect off-diagonal elements in M_{rb}, hence the inertia tensor is

$$M_{rb} = \text{diag}\,(m,\, m,\, m,\, I_x,\, I_y,\, I_z)\,, \tag{3}$$

where m is the mass of the ROV and I_x, I_y, and I_z represent the inertia along the front, right, and down body-fixed axes, respectively. Rigid-body Coriolis ($C_{rb}(\nu)$) and centripetal ($C_{rb}(\nu)$) matrices are given by

$$C_{rb}(\nu) = \begin{bmatrix} 0 & -mS(v^b) \\ -mS(v^b) & -S(\bar{J}\omega) \end{bmatrix},\; C_a(\nu) = \begin{bmatrix} 0 & S(v_1) \\ S(v_1) & S(v_2) \end{bmatrix}, \tag{4}$$

where $\bar{J} = \text{diag}(I_x, I_y, I_z)$, $S(\cdot)$ is the conventional skew-symmetric matrix, and

$$v_1 = col(X_{\dot{u}}u, Y_{\dot{v}}v, Z_{\dot{w}}w),\;\; v_2 = col(K_{\dot{p}}p, M_{\dot{q}}q, N_{\dot{r}}r), \tag{5}$$

with the parameters therein to be identified. The added mass inertia matrix is

$$M_a = \text{diag}(-X_{\dot{u}}, -Y_{\dot{v}}, -Z_{\dot{w}}, -K_{\dot{p}}, -M_{\dot{q}}, -N_{\dot{r}}), \tag{6}$$

where the coefficients need to be identified. The hydrodynamic damping matrix (Fossen, 1994) is approximated as $D(\nu) = D_l(\nu) + D_{nl}(\nu)$, where

$$D_l(\nu) = -\text{diag}\,(X_u,\, Y_v,\, Z_w,\, K_p,\, M_q,\, N_r) \tag{7}$$

$$\begin{aligned} D_{nl}(\nu) = -\text{diag}\,\big(&X_{u|u|}\,|u|\,,\, Y_{v|v|}\,|v|\,,\, Z_{w|w|}\,|w|\,, \\ &K_{p|p|}\,|p|\,,\, M_{q|q|}\,|q|\,,\, N_{r|r|}\,|r|\,\big)\,, \end{aligned} \tag{8}$$

with coefficients to be identified. Denoting with b the magnitude of the buoyant force, mg the magnitude of the gravitational force, g the gravitational acceleration, and x_b, y_b, and z_b the coordinates of the center of buoyancy in the body-fixed frame, the restoring forces and moments due to gravity and buoyancy can be modeled as

$$\begin{aligned} g(\eta) &= -\begin{bmatrix} f_g(\eta) + f_b(\eta) \\ r_g \times f_g(\eta) \end{bmatrix},\;\; r_g = col(x_b, y_b, z_b), \\ f_g(\eta) &= R_b^e(\eta)^T col(0, 0, mg),\;\; f_b(\eta) = -R_b^e(\eta)^T col(0, 0, b) \end{aligned} \tag{9}$$

2.1 Marine Current

To consider the current-induced forces and moments, it is sufficient to replace ν in (2) with the relative velocity $\nu_r = \nu - \nu_c$ (see Fossen (1994)), where $\nu_c = col(u_c, v_c, w_c, 0, 0, 0)$ is the (irrotational) marine current velocity expressed in the body-fixed frame. The ROV model (2) is

$$\dot{\eta} = J(\eta)\nu \tag{10}$$

$$M\dot{\nu} = \tau - g(\eta) - C(\nu_r)\nu_r - D(\nu_r)\nu_r + M\dot{\nu}_c, \tag{11}$$

where $C(\nu_r) = C_{rb}(\nu_r) + C_a(\nu_r)$ and $M = M_{rb} + M_a$.

2.2 Control Inputs

The wrench τ directly depends on the propulsion system. In this paper the BlueROV 2 Heavy (Wu, 2018) is taken as a case study, which is composed by $n_a = 8$ actuators, being able to provide the spinning thrusts $u_1, \ldots, u_8 \in \mathbb{R}$. The propulsion wrench τ is then $\tau = Fu$, where $u = col(u_1, \ldots, u_8)$ is taken as control input,

$$F = \begin{bmatrix} l_1 & \ldots & l_8 \\ r_1 \times l_1 & \ldots & r_8 \times l_8 \end{bmatrix} \in \mathbb{R}^{6\times8}, \tag{12}$$

determines the input mapping, where $l_1, \ldots, l_8 \in \mathbb{R}^3$ represents the unit vectors in the direction of the thrust, and $r_1, \ldots, r_8 \in \mathbb{R}^3$ are the vectors connecting the center of mass with the actuators.

3. DISTURBANCE OBSERVER

To achieve marine current compensation, we propose a NDO to estimate the effects of the unknown marine current on the system's dynamics. In this Section, we provide an overview of the NDO design and establish guaranteed bounds for the estimation errors.

3.1 Design

The ROV model (10)-(11) can be rewritten as

$$\dot{\eta} = J(\eta)\nu \tag{13}$$

$$M_{rb}\dot{\nu} = -g(\eta) + \tau + d(\nu, \nu_c, \dot{\nu}_c), \tag{14}$$

where the matching disturbance

$$d(\nu, \dot{\nu}, \nu_c, \dot{\nu}_c) = -M_a\dot{\nu} - C(\nu_r)\nu_r - D(\nu_r)\nu_r + M\dot{\nu}_c \tag{15}$$

lumps all the thrusts and torques, with the exception of those proved by actuators, gravity, and buoyancy. In other terms, the disturbance $d(\nu, \dot{\nu}, \nu_c, \dot{\nu}_c)$ contains all the unknown quantities that depend on the marine current, hence often unknown.

Although the disturbance depends from the motion of both the marine vessel and the marine current, it is overall time dependent, i.e., denoting the time t explicitly for once, we have $d(t) = d(\nu(t), \dot{\nu}(t), \nu_c(t), \dot{\nu}_c(t))$, or simply d. Since every involved variable is smooth, defining $\zeta = col(d, \dot{d}, \ldots, d^{(r-1)}) \in \mathbb{R}^{(6r)}$ it is possible to rewrite the disturbance d as the output of the exogenous system

$$\dot{\zeta} = A\zeta + Bd^{(r)},\;\; d = C\zeta, \tag{16}$$

where $d^{(r)}$ is smooth, and the matrices $A \in \mathbb{R}^{(6r)\times(6r)}$, $B \in \mathbb{R}^{(6r)\times 6}$ and $C = \in \mathbb{R}^{6\times(6r)}$ are given as

$$A = \begin{bmatrix} 0_6 & I_6 & & \\ \vdots & & \ddots & \\ 0_6 & & & I_6 \\ 0_6 & 0_6 & \dots & 0_6 \end{bmatrix} \quad B = \begin{bmatrix} 0_6 \\ \vdots \\ 0_6 \\ I_6 \end{bmatrix} \quad C = [I_6 \ 0_6 \ \dots \ 0_6]. \quad (17)$$

For $r = 1$, we have $A = 0_6$, $B = I_6$ and $C = I_6$. Note that the pair (A, B) is controllable and the pair (C, A) is observable for any positive integer r.

Under the previous restatement, a NDO (Li et al., 2014) is here designed in order to get an estimation $\hat{d}$ of d. To this end, consider the auxiliary variable $s = \zeta - HM_{rb}\nu$, where H is a matrix to design. By differentiation, we have

$$\dot{s} = (A - HC)s + AHM_{rb}\nu - H[-g(\eta) + Fu + CHM_{rb}\nu] + Bd^{(r)}. \quad (18)$$

Consider the disturbance observer

$$\dot{\hat{s}} = (A - HC)\hat{s} + AHM_{rb}\nu - H[-g(\eta) + Fu + CHM_{rb}\nu]$$
$$\hat{d} = C(\hat{s} + HM_{rb}\nu), \quad (19)$$

where $\hat{s}$ and $\hat{d}$ represent the estimations of s and d, respectively. Considering the error variables $\tilde{d} = d - \hat{d}$ and $\tilde{s} = s - \hat{s}$, we have the error system

$$\dot{\tilde{s}} = (A - HC)\tilde{s} + Bd^{(r)}, \ \ \tilde{d} = C\tilde{s},$$

which is linear time invariant and bounded input-bounded output whenever H is designed such that $A - HC$ is Hurwitz. Note that if $d^{(r)} = 0$ (i.e., the lumped disturbance is well approximated by a polynomial of order at most $r - 1$), the estimation error $\tilde{d}$ converges to zero asymptotically.

3.2 Bound Analysis

Since we have assumed that the ROV and the marine current have relatively slow dynamics, it is reasonable to assume that d has dominant low frequencies, and therefore the r-time derivative $d^{(r)}$ is bounded. More precisely, we assume $\left\|d^{(r)}\right\| \leq \rho$, for some $\rho \geq 0$, eventually unknown. For example, piece-wise signals and swept lines have null second order derivative almost everywhere, and not rarely tracking references are provided slow varying, trapezoidal, or constant.

Let us denote $\bar{A} = (A - HC)$. Consider the Lyapunov function $V = \tilde{s}^T P \tilde{s}$, where P is symmetric and positive definite. We have

$$\dot{V} = 2\tilde{s}^T P\bar{A}\tilde{s} + 2\tilde{s}^T Bd^{(r)} = \tilde{s}^T(\bar{A}^T P + P\bar{A})\tilde{s} \quad (20)$$
$$+ 2\tilde{s}^T Bd^{(r)} = -\tilde{s}^T Q\tilde{s} + 2\tilde{s}Bd^{(r)}. \quad (21)$$

where $\bar{A}^T P + P\bar{A} = -Q$, with Q symmetric and positive definite, which leads to $\dot{V} \leq -\lambda_{min}(Q)\left\|\tilde{s}\right\|^2 + 2\rho\left\|\tilde{s}\right\|$, where $\lambda_{min}(Q) > 0$ denotes the minimum eigenvalue of Q, and $\left\|Bd^{(r)}\right\| = \left\|d^{(r)}\right\|$. It follows that the estimation error system is ultimately bounded (see Khalil (2002)), with ultimate bound of $\|\tilde{s}\|$ equal to $\frac{2\rho}{\lambda_{min}(Q)}$. It follows that the ultimate bound of $\left\|\tilde{d}\right\|$ is equal to $\|C\|\frac{2\rho}{\lambda_{min}(Q)}$.

4. CONTROL

In this Section, we show how to leverage the disturbance estimation from Section 3 to perform disturbance compensation. Firstly, we present the control law design. Then, we discuss the boundedness of the tracking error in closed loop.

4.1 Design

The DOBC scheme (Li et al., 2014) is completed with a feedback linearization composite controller. The estimation $\hat{d}$ of d is then fed-forward in order to counteract the effect of the unknown wrench.

Consider the variables $\xi_1 = \eta$ and $\xi_2 = J(\eta)\nu$, which let us to rewrite the ROV model (13) as

$$\dot{\xi}_1 = \xi_2 \quad (22)$$
$$\dot{\xi}_2 = \dot{J}(\eta)\nu + J(\eta)M_{rb}^{-1}(-g(\eta) + Fu + \hat{d} + \tilde{d}). \quad (23)$$

The term $\dot{J}(\eta)$ is the component-wise time differentiation of $J(\eta)$, whose calculation involves kinematics only and it is not directly affected by the disturbance d.

Let η_{1r} be the tracking reference for η. The control law is

$$u = F^{+}\tau_c \quad (24)$$
$$\tau_c = g(\eta) - \hat{d} + M_{rb}J^{-1}(\eta)(-\dot{J}(\eta)\nu + v), \quad (25)$$

where F^{+} is any left inverse of F and the vector v is a new input designed as

$$v = \ddot{\eta}_r - K_1(J(\eta)\nu - \dot{\eta}_r) - K_0(\eta - \eta_r), \quad (26)$$

where $K_1, K_2 \in \mathbb{R}^{6\times 6}$ are design parameters. In this work, the left inverse of F is employed for simplicity; however, several strategies have been proposed in the literature to solve this so-called control allocation problem (Johansen and Fossen, 2013), including, for example, the capability to manage saturation constraints (Baldini et al., 2018b) or actuator faults (Baldini et al., 2017). The closed loop system is

$$\dot{\xi}_1 = \xi_2 \quad (27)$$
$$\dot{\xi}_2 = \ddot{\xi}_{1r} - K_1(\xi_2 - \dot{\xi}_{1r}) - K_0(\xi_1 - \xi_{1r}) + J(\eta)M_{rb}^{-1}\tilde{d}. \quad (28)$$

Defining the error variables $e_1 = \eta - \eta_r$ and $e_2 = J(\eta)\nu - \dot{\eta}_r$, we have the error system

$$\dot{e}_1 = e_2, \quad \dot{e}_2 = -K_0 e_1 - K_1 e_0 + J(\eta)M_{rb}^{-1}\tilde{d}. \quad (29)$$

The estimation error $\tilde{d}$ affects the error system in a matching way, as expected. In case of perfect disturbance estimation ($\tilde{d} = 0$) the provided law solves tracking problem, accomplishing a static full state feedback linearization (Nijmeijer and Van der Schaft, 1990). The effect of $\tilde{d}$ is however not negligible in general.

4.2 Closed Loop

Summing up both the tracking error and the observer, we have the overall closed loop error system

$$\begin{bmatrix} \dot{e}_1 \\ \dot{e}_2 \\ \dot{\tilde{s}} \end{bmatrix} = \begin{bmatrix} 0 & I & 0 \\ -K_0 & -K_1 & J(\eta)M_{rb}^{-1}C \\ 0 & 0 & (A - HC) \end{bmatrix} \begin{bmatrix} e_1 \\ e_2 \\ \tilde{s} \end{bmatrix} + \begin{bmatrix} 0 \\ 0 \\ B \end{bmatrix} d^{(r)}. \quad (30)$$

Provided the previously discussed for the choice of H, K_1 and K_2, the overall tracking error is input to state stable with respect to $d^{(r)}$. Note that in case of $d^{(r)} = 0$, the discussed overall law solves the asymptotic disturbance decoupling problem (Andiarti and Moog, 1996). The tracking DOBC scheme is reported in Figure 1.

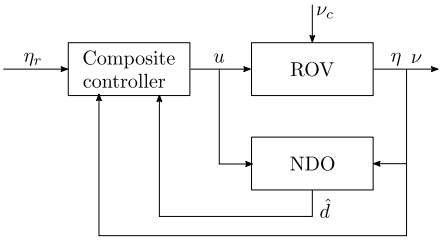

Fig. 1. DOBC scheme.

4.3 Parameter tuning

We note from (30) that the error dynamics matrix is block triangular, so the disturbance estimation error is independent of the tracking error, in accordance with the separation principle. As a consequence, H can be tuned independently, simplifying the tuning stage. As a rule of thumb, the estimation error should have faster dynamics, while the tracking error dynamics should be slower to avoid actuator wear-and-tear. Furthermore, the farther the poles of the estimation errors from the imaginary axis, the quicker the convergence and the greater the susceptibility to sensor noise. So, H is chosen to locate stable poles, trading-off convergence speed with sensor noise mitigation. Then, K_1 and K_2 can be designed to locate the remaining poles closer to the imaginary axis.

5. NUMERICAL SIMULATION

The proposed DOBC scheme is tested in simulation using the Matlab Simulink. The sample time is set as $T_c = 10^{-3}$ s, for a total time of 60 s. We test the DOBC strategy for the ROV on a six degrees of freedom position and attitude tracking problem. The full set of parameters represents a BlueROV 2 Heavy (Wu, 2018) and it is reported in Table 1. Control law parameters and NDO parameters are instead reported in Table 2. All the control law parameters are the outcome of a grid search tuning phase.

The tracking reference (denoted by subscript r in the following figures for clarity) is composed by two square trajectories in the (x, y) plane. The first square has side equal to 5 m and travel time of 30 s, while the subsequent square has side equal to 3 m and travel time of 25 s. The

Table 1. ROV constructive and hydrodynamic parameters (Wu, 2018) in SI units.

Par.	Value	Par.	Value	Par.	Value
m	11.5	Y_v	-6.22	$Z_{w\|w\|}$	-36.99
b	114.777	Z_w	-5.18	K_p, M_q, N_r	-0.07
$X_{\dot{u}}$	-5.5	x_b, y_b	0	I_x, I_y, I_z	0.16
$Y_{\dot{v}}$	-12.7	z_b	-0.02	$K_{\dot{p}}, M_{\dot{q}}, N_{\dot{r}}$	-0.12
$Z_{\dot{w}}$	-14.57	$X_{u\|u\|}$	-18.18	$K_{p\|p\|}, M_{q\|q\|}, N_{r\|r\|}$	-1.55
X_u	-4.03	$Y_{v\|v\|}$	-21.66		

Table 2. Design parameters.

Description	Value
x and y closed loop poles	$-1, -2$
z closed loop poles	$-1, -2$
φ and θ closed loop poles	$-1, -2$
ψ closed loop poles	$-1, -2$
Observer order (r)	3
$\sigma(A - HC)$	$-10, \ldots, -10$

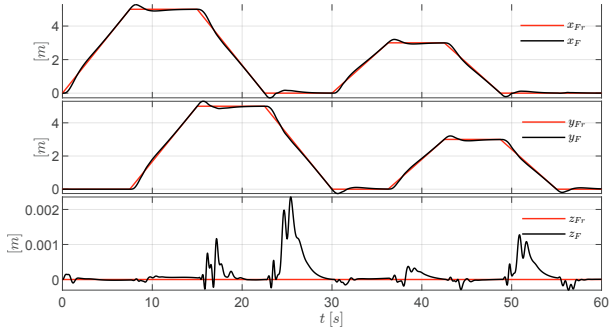

Fig. 2. Position.

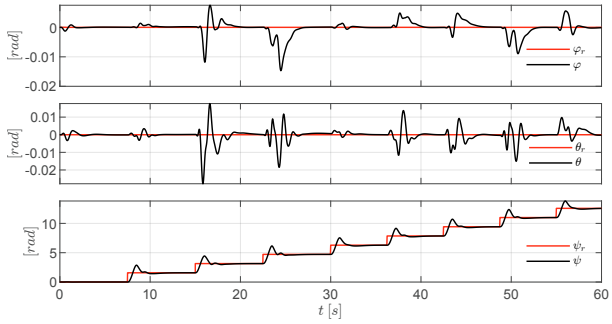

Fig. 3. Attitude.

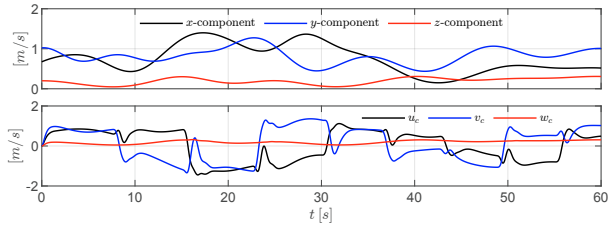

Fig. 4. Marine current velocity in the earth fixed frame (above) and in the body fixed frame (bottom).

yaw angle is increased in order to keep the orientation tangent to the trajectory. The linear position performances are reported in Fig. 2, where the red line represents the reference and the black line is the actual state. The reference is composed by a combination of ramps, which is then filtered through a second order system. The angular performances are reported in Fig. 3. In the both linear and angular components, the solution is able to solve the tracking problem even in the presence of the unknown lumped disturbance d.

The simulated marine current velocity components are reported in Figure 4 for both the earth frame and the body frame. Note that each velocity component is smooth and quite slow varying. The lumped disturbance d is instead reported in Figure 5 and in Figure 6, together with its estimation provided by the NDO. It can be noticed that the NDO is able to get an estimation of d with reasonable bound.

5.1 The effect of the NDO estimation

The proposed DOBC technique is compared with a standard static feedback linearization, providing a fair comparison to understand the role of the NDO. To achieve static feedback linearization, $\hat{d} = 0$ is enforced in the

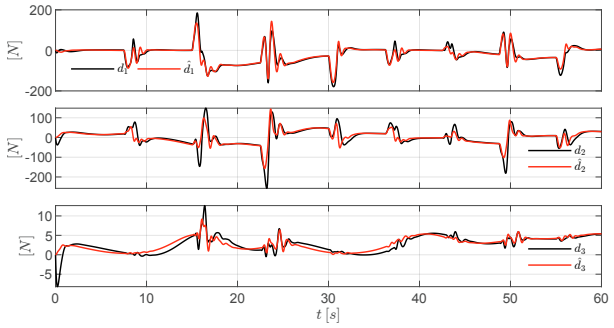

Fig. 5. Actual and estimated lumped disturbances.

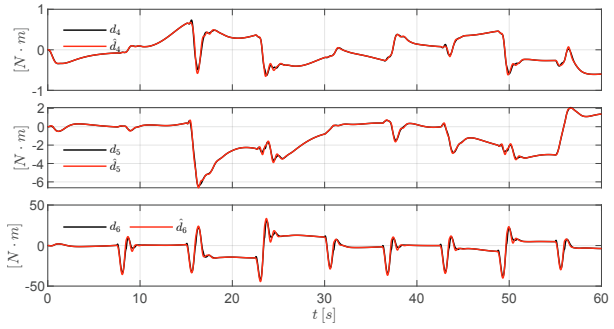

Fig. 6. Actual and estimated lumped disturbances.

proposed scheme, while the rest of the control loop is unchanged. All the simulation parameters and settings remain identical, including the controller parameters. As the original solution for the Dynamic Position problem is based on three decoupled PIDs (Fossen, 2000), we also include a comparison with a PID-based solution. To make the comparison between a linear PID-based control strategy and the proposed nonlinear strategy fair, we refine the PID-based approach, employing a feedback linearization approach to actually decouple the inputs, and then the static allocation is replaced by a PID auxiliary controller (FL + PID, i.e., PIDs replacing v in (26)). The overall plot in the (x, y) plane is reported in Figure 7. It can

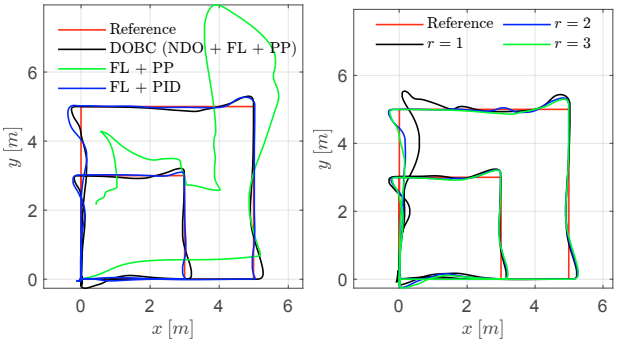

Fig. 7. Position in the (x, y) plane for the DOBC solution, the Feedback Linearization (FL), and the FL with PID, and for DOBC with increasing NDO orders r.

be noticed how the feedback linearization is not able to follow the tracking reference. This could have been expected, since although the disturbance d is composed by low frequencies, it can be noticeable in the magnitude. The parameters of the PID controllers have been set according to a pole placement, where two poles are the same as in Table 2, while the additional ones are -10 for position

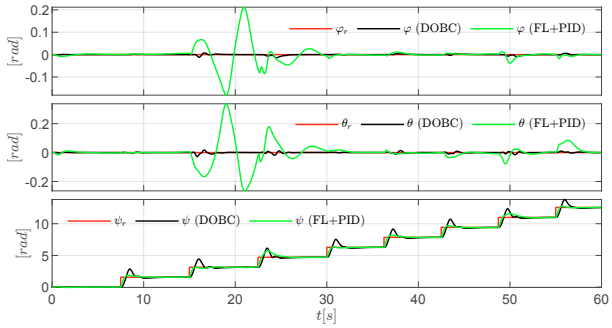

Fig. 8. Attitude in the (x, y) plane for the DOBC and the Feedback Linearization with PID (FL + PID).

control and -30 for attitude control. The advantage of the DOBC over FL is clear, since the role of the NDO is that of providing an additional feed-forward action leading to the disturbance attenuation. Instead, FL + PID performs similarly to DOBC in the linear position (see Figure 7), while FL + PID shows a larger error in φ and θ during aggressive maneuvers (see Figure 8). It is remarkable that, even if the composite controller is a static one, the overall DOBC is a dynamic controller, i.e., a model-based dynamic compensator, as well as the FL + PID scheme.

5.2 The effect of the NDO order

The DOBC is composed by a feedback linearization and a NDO, and it is therefore a dynamic control algorithm. In case the order of the NDO is $r = 1$, for each component of d we have an additional model-based integral action. However, the increasing of the order r leads to additional integral actions, whose effects are compared in Figure 7.

6. CONCLUSION

In this paper, a DOBC scheme is presented to address the trajectory tracking problem for a BlueROV 2 Heavy. The result is a nonlinear dynamic compensator that includes a feed-forward action, providing disturbance attenuation against a matching lumped disturbance. In the control law design, only constructive parameters are utilized, while the effects of all remaining contributions, dependent on potentially unknown parameters, are lumped and estimated by the disturbance observer. Despite the presence of nonlinear terms in the model and the control laws, the observer and the overall closed loop result in linear time-invariant systems, with both estimations and tracking errors bounded. As demonstrated by numerical simulations, increasing the order r of the NDO provides additional feed-forward integral actions. In our future work, we are investigating the benefits of higher-order composite controllers in the case of time-varying marine currents. Additionally, to validate the proposed method in a real-world system implementation, we are exploring the integration of loop shaping techniques into the control law design to perform wave filtering for reducing high-frequency actuator thrust ripples.

REFERENCES

Ahmed, N., Chen, M., and Shao, S. (2020). Disturbance observer based tracking control of quadrotor with high-order disturbances. *IEEE access*, 8, 8300–8313.

Andiarti, R. and Moog, C.H. (1996). Output feedback disturbance decoupling in nonlinear systems. *IEEE transactions on automatic control*, 41(11), 1683–1689.

Baldini, A., Ciabattoni, L., Felicetti, R., Ferracuti, F., Monteriù, A., Fasano, A., and Freddi, A. (2017). Active fault tolerant control of remotely operated vehicles via control effort redistribution. In *Volume 9: 13th ASME/IEEE International Conference on Mechatronic and Embedded Systems and Applications*, International Design Engineering Technical Conferences and Computers and Information in Engineering Conference, V009T07A002. Cleveland, Ohio, USA.

Baldini, A., Ciabattoni, L., Felicetti, R., Ferracuti, F., Freddi, A., and Monteriù, A. (2018a). Dynamic surface fault tolerant control for underwater remotely operated vehicles. *ISA transactions*, 78, 10–20.

Baldini, A., Fasano, A., Felicetti, R., Freddi, A., Longhi, S., and Monteriù, A. (2018b). A constrained thrust allocation algorithm for remotely operated vehicles. *IFAC-PapersOnLine*, 51(29), 250–255.

Baldini, A., Felicetti, R., Freddi, A., Longhi, S., and Monteriù, A. (2022a). Actuator fault tolerant control via active fault diagnosis for a remotely operated vehicle. *IFAC-PapersOnLine*, 55(6), 310–316.

Baldini, A., Felicetti, R., Freddi, A., Longhi, S., and Monteriù, A. (2022b). Fault tolerant control for remotely operated vehicles with thruster faults using nonlinear disturbance observers. *IFAC-PapersOnLine*, 55(31), 275–280.

Benevides, J.R., Paiva, M.A., Simplício, P.V., Inoue, R.S., and Terra, M.H. (2022). Disturbance observer-based robust control of a quadrotor subject to parametric uncertainties and wind disturbance. *IEEE Access*, 10, 7554–7565.

Chen, W.H., Yang, J., Guo, L., and Li, S. (2016). Disturbance-observer-based control and related methods—an overview. *IEEE Transactions on Industrial Electronics*, 63(2), 1083–1095.

Chen, Z., Zhang, Y., Zhang, Y., Nie, Y., Tang, J., and Zhu, S. (2019). Disturbance-observer-based sliding mode control design for nonlinear unmanned surface vessel with uncertainties. *IEEE Access*, 7, 148522–148530.

Chu, Z., Chen, Y., Zhu, D., and Zhang, M. (2021). Observer-based adaptive neural sliding mode trajectory tracking control for remotely operated vehicles with thruster constraints. *Transactions of the Institute of Measurement and Control*, 43(13), 2960–2971.

Chu, Z., Zhu, D., and Eu Jan, G. (2016). Observer-based adaptive neural network control for a class of remotely operated vehicles. *Ocean Engineering*, 127, 82–89.

Cui, R., Chen, L., Yang, C., and Chen, M. (2017). Extended state observer-based integral sliding mode control for an underwater robot with unknown disturbances and uncertain nonlinearities. *IEEE Transactions on Industrial Electronics*, 64(8), 6785–6795.

Fossen, T.I. (2000). A survey on nonlinear ship control: From theory to practice. *IFAC Proceedings Volumes*, 33(21), 1–16.

Fossen, T. (1994). *Guidance and Control of Ocean Vehicles*. Wiley.

Gao, J., Zhang, G., Wu, P., Zhao, X., Wang, T., and Yan, W. (2019). Model predictive visual servoing of fully-actuated underwater vehicles with a sliding mode disturbance observer. *IEEE Access*, 7, 25516–25526.

Gu, N., Wang, D., Peng, Z., Wang, J., and Han, Q.L. (2022). Disturbance observers and extended state observers for marine vehicles: A survey. *Control Engineering Practice*, 123, 105158.

Guerrero, J., Torres, J., Creuze, V., and Chemori, A. (2020). Adaptive disturbance observer for trajectory tracking control of underwater vehicles. *Ocean Engineering*, 200, 107080.

Guo, B.Z. and Zhao, Z.l. (2011). On the convergence of an extended state observer for nonlinear systems with uncertainty. *Systems & Control Letters*, 60(6), 420–430.

Guo, L. and Chen, W.H. (2005). Disturbance attenuation and rejection for systems with nonlinearity via dobc approach. *International Journal of Robust and Nonlinear Control: IFAC-Affiliated Journal*, 15(3), 109–125.

Hosseinnajad, A. and Loueipour, M. (2021). Design of finite-time active fault tolerant control system with real-time fault estimation for a remotely operated vehicle. *Ocean Engineering*, 241.

Hosseinnajad, A. and Loueipour, M. (2023). Fault tolerant control system for an rov based on a novel integral sliding mode control and a state and fault observer in the presence of thruster limitations. *Ocean Engineering*, 280, 114687.

Johansen, T.A. and Fossen, T.I. (2013). Control allocation—a survey. *Automatica*, 49(5), 1087–1103.

Khalil, H. (2002). *Nonlinear Systems*. Pearson Education. Prentice Hall.

Li, S., Yang, J., Chen, W.H., and Chen, X. (2014). *Disturbance observer-based control: methods and applications*. CRC press.

Li, X., Zhao, M., and Ge, T. (2018). A nonlinear observer for remotely operated vehicles with cable effect in ocean currents. *Applied Sciences*, 8(6), 867.

Liu, X., Zhang, M., Wang, Y., and Rogers, E. (2018). Design and experimental validation of an adaptive sliding mode observer-based fault-tolerant control for underwater vehicles. *IEEE Transactions on Control Systems Technology*, 27(6), 2655–2662.

Mu, W., Wang, Y., Sun, H., and Liu, G. (2021). Double-loop sliding mode controller with an ocean current observer for the trajectory tracking of rov. *Journal of Marine Science and Engineering*, 9(9), 1000.

Nijmeijer, H. and Van der Schaft, A. (1990). *Nonlinear dynamical control systems*, volume 464. Springer.

Oliveira, É.L., Orsino, R.M., and Donha, D.C. (2021). Disturbance-observer-based model predictive control of underwater vehicle manipulator systems. *IFAC-PapersOnLine*, 54(16), 348–355.

Walker, K.L., Gabl, R., Aracri, S., Cao, Y., Stokes, A.A., Kiprakis, A., and Giorgio-Serchi, F. (2021). Experimental validation of wave induced disturbances for predictive station keeping of a remotely operated vehicle. *IEEE Robotics and Automation Letters*, 6(3), 5421–5428.

Wu, C.J. (2018). *6-dof modelling and control of a remotely operated vehicle*. Ph.D. thesis, Flinders University, College of Science and Engineering.

Yang, J., Li, S., and Yu, X. (2012). Sliding-mode control for systems with mismatched uncertainties via a disturbance observer. *IEEE Transactions on industrial electronics*, 60(1), 160–169.